

## Supporting information

### **Ag-Ru interface for highly efficient hydrazine assisted water electrolysis**

Xiaoyang Fu<sup>a</sup>, Dongfang Cheng<sup>b</sup>, Ao Zhang<sup>c</sup>, Jingxuan Zhou<sup>a</sup>, Sibowang<sup>a</sup>, Xun Zhao<sup>d</sup>, Jun Chen<sup>d</sup>, Philippe Sautet<sup>ab, \*</sup>, Yu Huang<sup>c, \*</sup> and Xiangfeng Duan<sup>a, \*</sup>

<sup>a</sup>Department of Chemistry and Biochemistry, University of California, Los Angeles, Los Angeles, CA 90095, USA. Email: xduan@chem.ucla.edu

<sup>b</sup>Department of Chemical and Biomolecular Engineering, University of California, Los Angeles, Los Angeles, CA 90095, USA. Email: sautet@ucla.edu

<sup>c</sup>Department of Materials Science and Engineering, University of California, Los Angeles, Los Angeles, CA 90095, USA. Email: yhuang@seas.ucla.edu

<sup>d</sup>Department of Bioengineering, University of California, Los Angeles, Los Angeles, CA 90095, USA.

## Experimental Section

### Chemicals

Silver nitrate ( $\text{AgNO}_3$ , analytical grade), Ruthenium chloride hydrate ( $\text{RuCl}_3 \cdot x\text{H}_2\text{O}$ , 38.0% - 42.0% Ru basis), polyvinylpyrrolidone (PVP, MW  $\sim 55,000$ ), hydrazine solution (35 wt% in water) and commercial Ru/C (5%) were all purchased from Sigma-Aldrich. Carbon paper (Freudenberg H27) and anion exchange membrane (AEM) (FAS-50) were purchased from the fuelcell store. The electrolyzer and the electric pump were purchased from Gauss Union as shown in Fig. S17.

### Synthesis

The synthesis of Ru decorated Ag NPs was achieved via a facile polyol method. 160 mg of PVP was dissolved in 4 ml ethylene glycol and then aqueous solutions of 0.024 mmol  $\text{AgNO}_3$  and 0.012 mmol  $\text{RuCl}_3 \cdot x\text{H}_2\text{O}$  were added, respectively. After ultra-sonication, the vial was heated at 225 °C for 4 h and followed by the post-synthetic washing/centrifuging with water/acetone and ethanol/acetone. The final products were re-dispersed in ethanol. For comparison, the ultrasmall Ru NPs are synthesized without the addition of  $\text{AgNO}_3$ .

### Characterization

The transmission electron microscopy (TEM) was carried out on FEI T12 transmission electron microscope operated at 120 kV. The X-ray diffraction (XRD) was carried out on a Panalytical X'Pert Pro X-ray Powder Diffractometer with  $\text{Cu-K}\alpha$  radiation. X-ray photoelectron spectroscopy (XPS) was carried out with Kratos AXIS Ultra DLD spectrometer. The XPS are calibrated based on adventitious C (284.6 eV). The scanning transmission electron microscope (STEM) image and energy dispersive x-ray spectroscopy (EDX) mapping were carried out on Joel Jem-300CF (Grand Arm) operated at 300 kV. The inductively coupled plasma-atomic emission spectroscopy (ICP-AES) was carried out to determine the loading of the electrocatalysts.

### Electrochemical study

The electrochemical tests were carried out in a three-electrode cell system. The working electrode was an RDE with a geometric area of 0.196  $\text{cm}^2$  and the counter electrode was a graphite rod. The reference electrode was Hg/HgO (1.0 M KOH) and the potentials are calibrated and converted against reversible hydrogen electrode (RHE). The homogeneous ethanol dispersion of the electrocatalysts was dropcasted onto the RDE surface and dried under

room temperature with Ru loading of 1.0  $\mu\text{g}$  ( $5.1 \mu\text{g}/\text{cm}^2$ ) for the electrocatalysts. HzOR tests were carried out in Ar-saturated electrolyte of 1.0 M KOH, 5.0 mM hydrazine via linear sweep voltammetry (LSV) at a series of rotation rates of 225, 400, 625, 900, 1225 and 1600 rpm, with potential scan rate of 20 mV/s to study the electron transfer number. The HzOR was also tested on gas diffusion electrode with the loading of 1.0  $\mu\text{g}/\text{cm}^2$  in the electrolyte of 1.0 M KOH, 0.10 M hydrazine via LSV. The CA tests were carried out at 0.20 V vs. RHE for 1 h. The performances of HER were tested on RDE with electrocatalysts loading of 1.0  $\mu\text{g}$  ( $5.1 \mu\text{g}/\text{cm}^2$ ) via LSV in 1.0 M KOH electrolyte and CP was employed at geometric current density of 10  $\text{mA}/\text{cm}^2$  for 10 h to study the long-term performance. For the electrochemical performance metrics, the average value and the standard deviation from 3 tests were reported.

#### Hydrazine assisted water electrolysis

MEA process was carried out by sandwiching two carbon paper electrodes ( $1.0 \text{ cm}^2$ ,  $0.20 \text{ mg}_{\text{Ru}}$  loading for the electrocatalysts) with AEM and Teflon gaskets. Electric pumps were employed to circulate the anolyte (1.0 M KOH + 1.0 M hydrazine) and catholyte (1.0 M KOH) at the flow rate of  $\sim 80 \text{ mL}/\text{min}$ . LSV was conducted in the range from -0.1 V to 0.45 V at 2 mV/s for the polarization curves. CP was tested at 100  $\text{mA}/\text{cm}^2$  to study the long-term performances of the electrolyzer with periodically refreshing electrolyte and changing AEM. The hydrogen gas produced during electrolysis was collected via the water displacement method. For the detection of the potential byproduct ammonia,  $^1\text{H}$  NMR tests were carried on Bruker AVS400 instrument. For the sample preparation, the aliquots are added with concentrated hydrochloric acid (36%), DMSO- $d_6$ , and 10.0 mM 3-(Trimethylsilyl)propionic-2,2,3,3- $d_4$  acid sodium salt (internal standard) aqueous solution with a volumetric ratio of 4.00:1.00:5.00:1.11.

#### DFT Computation details

Vienna ab initio simulation package (VASP) was used to carry out all the periodic DFT calculations. The Perdew-Burke-Ernzerhof (PBE) parametrization of the generalized gradient approximation (GGA) of the exchange-correlation functional was employed<sup>[1]</sup>, along with the dDsC dispersion correction to account for van der Waals interaction<sup>[2]</sup>. The cut off energy is 400 eV. The interactions between the atomic cores and electrons were described by the projector augmented wave (PAW) method<sup>[3]</sup>. All structures were optimized until the force and energy on each atom was less than 0.02 eV/Å and  $10^{-6}$  eV, respectively. A dipole correction in the z direction was used for surface calculations. The transition state search was conducted with the

climbing image nudged elastic band (CI-NEB) method, followed by the dimer method to converge the saddle point within 0.05 eV/Å<sup>4</sup>].

The calculations of Gibbs free energies include thermal effects, zero point energies, and entropic contributions, where translational, rotational, and vibrational degrees of freedom were taken into account for gaseous species. For surface species, Harmonic Oscillator (HO) approximation was used and only vibrational contributions were considered. Using this approximation, we can calculate the internal energy (U) and entropy of the adsorbate as follows:

$$U(T) = E_{elec} + E_{ZPE} + \sum_i^{harm\ DOF} \frac{\epsilon_i}{e^{\epsilon_i/k_B T} - 1}$$

$$S = k_B \sum_i^{harm\ DOF} \left[ \frac{\epsilon_i}{k_B T (e^{\epsilon_i/k_B T} - 1)} - \ln(1 - e^{-\epsilon_i/k_B T}) \right]$$

Where,  $\epsilon_i$  are the harmonic energies for the adsorbate atoms.

The Helmholtz free energy (F) can hence be calculated as:

$$F(T) = U(T) - TS(T)$$

Assuming that the pV term in  $H = U + pV$  is negligible, the Helmholtz Free energy can be used as an approximate for the Gibbs Free energy since  $G \approx F$ .

Four-layer (4×3)-Ag(100), four-layer (4\*1)-Ru(1013) and three-layer (7\*4) Ag(100) supported Ru rod slabs were used in the calculations. For these periodicities, the Brillouin zone was sampled using (6 × 4 × 1), (4 × 6 × 1) and (1 × 2 × 1) Gamma-point-centered K-meshes, respectively. The bottom two layers are fixed while the upper layers and adsorbates were relaxed during optimization. The formation free energy ( $G_f$ ) of hydroxylated surface is calculated as:

$$G_f = G(\text{slab}(\text{OH})_x) + x\mu(\text{H}) - G(\text{clean}) - xG(\text{H}_2\text{O})$$

$$= G(\text{slab}(\text{OH})_x) + x(1/2G(\text{H}_2) - eU - \ln 10 k_B T \text{pH}) - G(\text{clean}) - xG(\text{H}_2\text{O})$$

Where U is the electrode potential at SHE scale. The pressures of H<sub>2</sub> and H<sub>2</sub>O are set as 1atm.

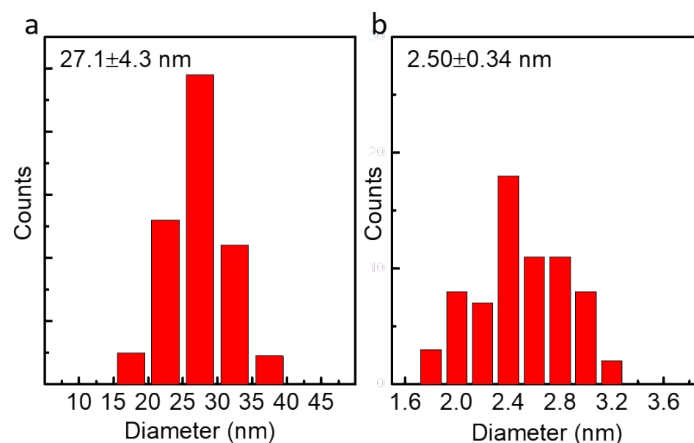


**Fig. S1** Size distributions of Ru NPs decorated Ag NPs. (a) Ag NPs. (b) Ru NPs.

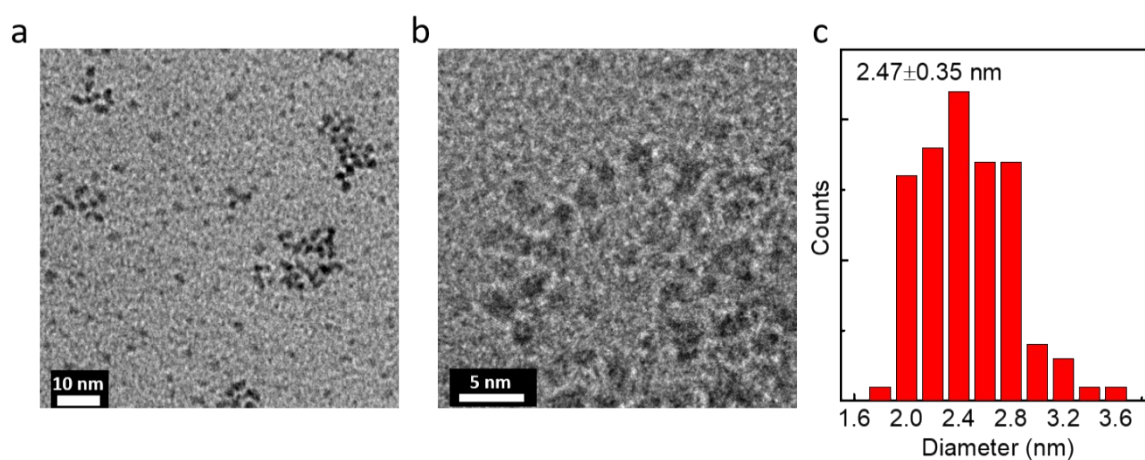


**Fig. S2** TEM (a), HRTEM (b) pictures and the size distributions (c) of ultrasmall Ru NPs.

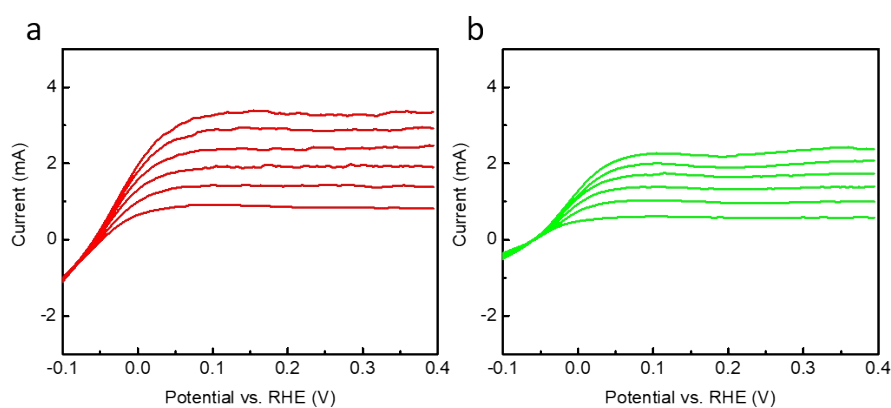


**Fig. S3** LSV curves of Ru decorated Ag NPs (a) and Ru NPs (b) in  $1.0$  M KOH +  $5.0$  mM hydrazine electrolyte at a various of rotation rates of 1600, 1225, 900, 625, 400, 225 rpm.

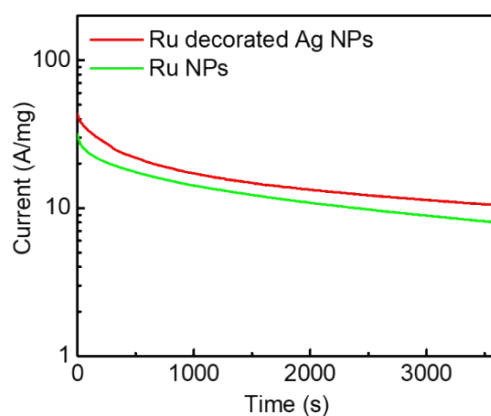


**Fig. S4** Chronoamperometry tests of Ru decorated Ag NPs and Ru NPs on carbon paper at 0.20 V vs. RHE in 1.0 M KOH+0.10 M hydrazine electrolyte.

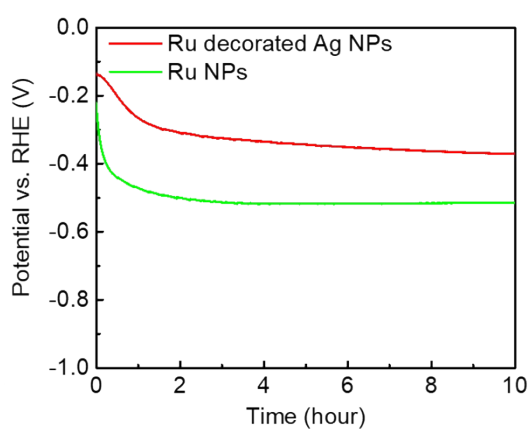


**Fig. S5** Chronopotentiometry tests of the Ru decorated Ag NPs and Ru NPs at 10 mA/cm<sup>2</sup> in 1.0 M KOH electrolyte at a rotation rate of 1600 rpm.

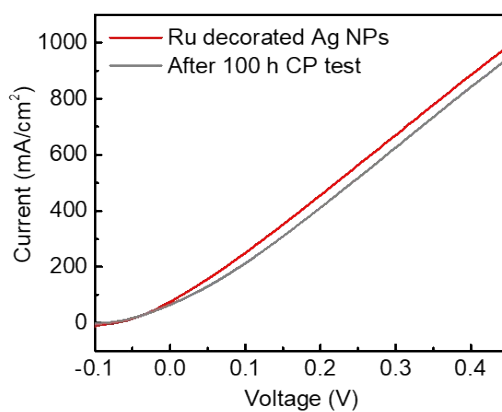


**Fig. S6** Performance of the hydrazine assisted water electrolysis before and after 100 h CP test.

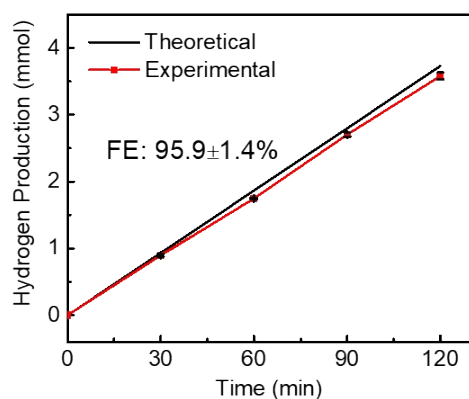


**Fig. S7** The amount of hydrogen production during electrolysis at 100 mA/cm<sup>2</sup> from theoretical calculation and experimental measurement.

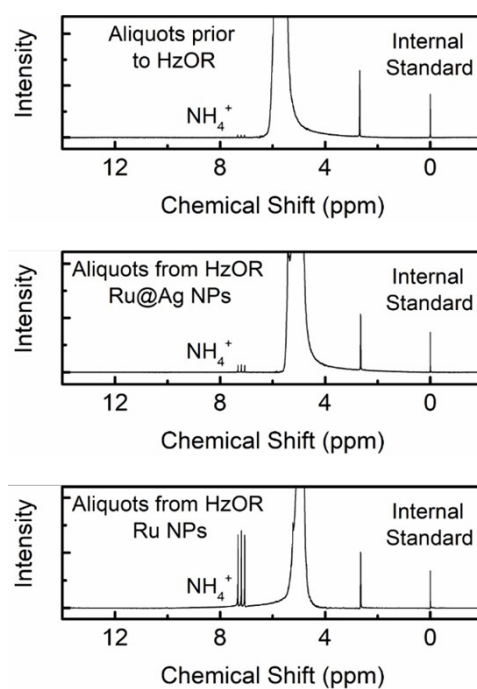


**Fig. S8** <sup>1</sup>H NMR tests of the acidified aliquots prior to HzOR test and from HzOR tests on Ru@Ag NPs (with little ammonia signal) and Ru NPs (with much more evident ammonia signal).

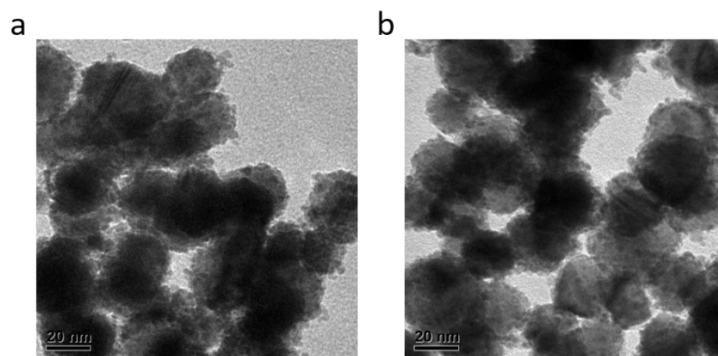


**Fig. S9** TEM pictures of anode electrocatalysts (a) after CP test and cathode electrocatalysts (b) after CP test.

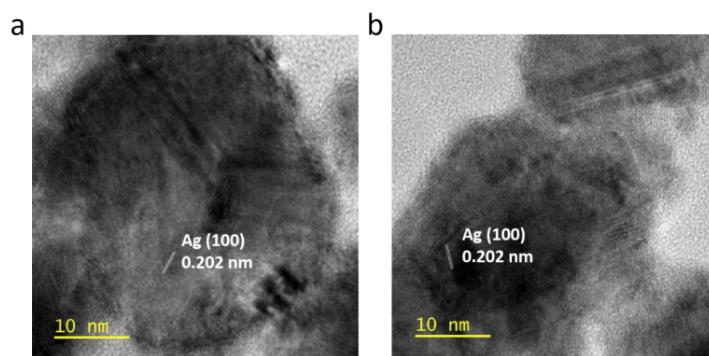


**Fig. S10** HRTEM picture of anode electrocatalysts (a) after CP test and cathode electrocatalysts (b) after CP test.

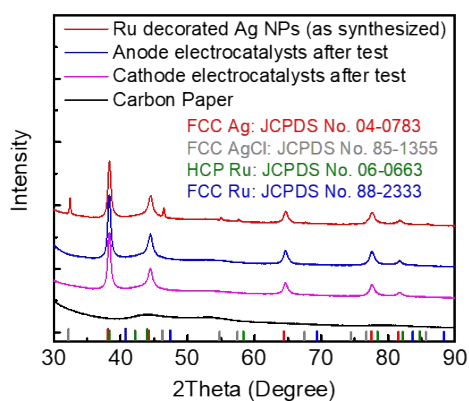


**Fig. S11** XRD of the as synthesized Ru decorated Ag NPs electrocatalysts, anode and cathode electrocatalysts after the CP test and the carbon paper.

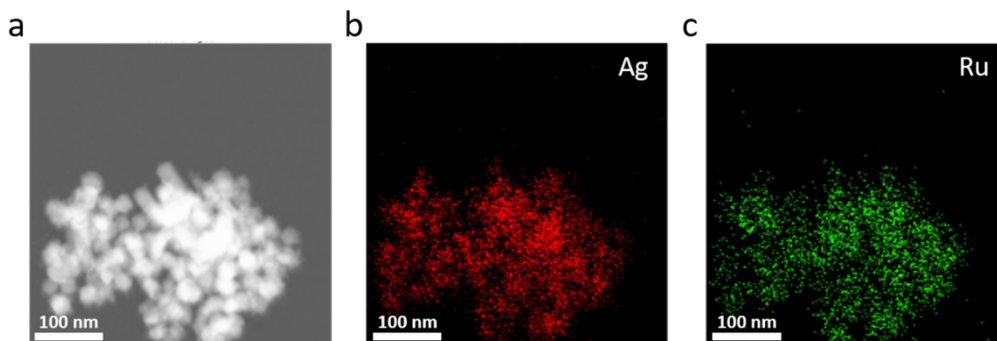


**Fig. S12** (a) STEM and EDS mapping of the anode electrocatalysts after CP test regarding Ag (b) and Ru (c) element.

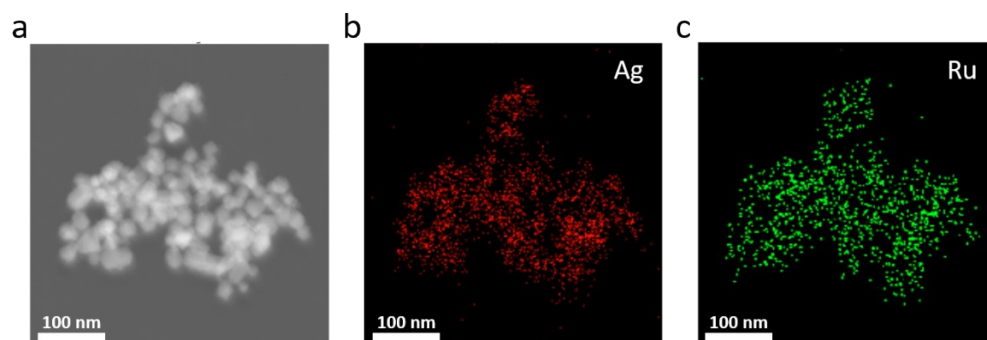


**Fig. S13** (a) STEM and EDS mapping of the cathode electrocatalysts after CP test regarding Ag (b) and Ru (c) element.

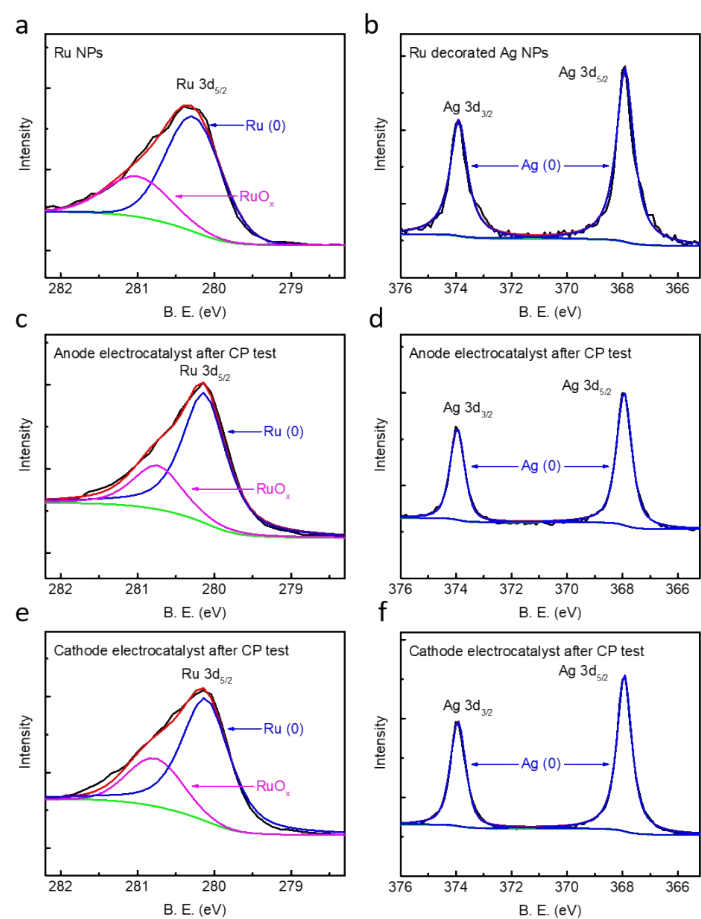


**Fig. S14** XPS study of the electrocatalysts. Electrocatalysts prior to CP test regarding Ru (a) and Ag (b) element. for Rh element. Anode electrocatalysts after CP test regarding Ru (c) and Ag (d) element. Cathode electrocatalysts after CP test regarding Ru (e) and Ag (f) element

Ru(1013)

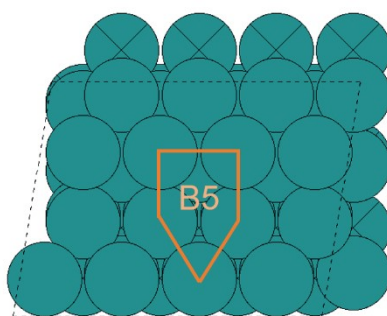


**Fig. S15** Illustration of the B5 site on Ru (1013).

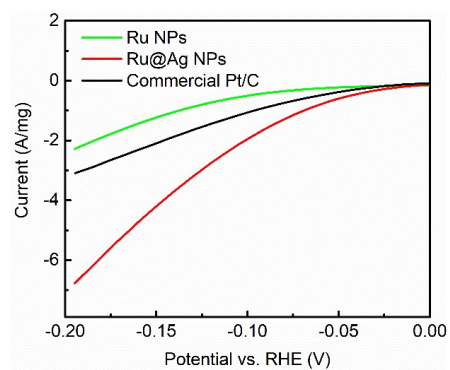


**Fig. S16** Comparison of commercial Pt/C with Ru@Ag NPs and Ru NPs regarding HER performance.

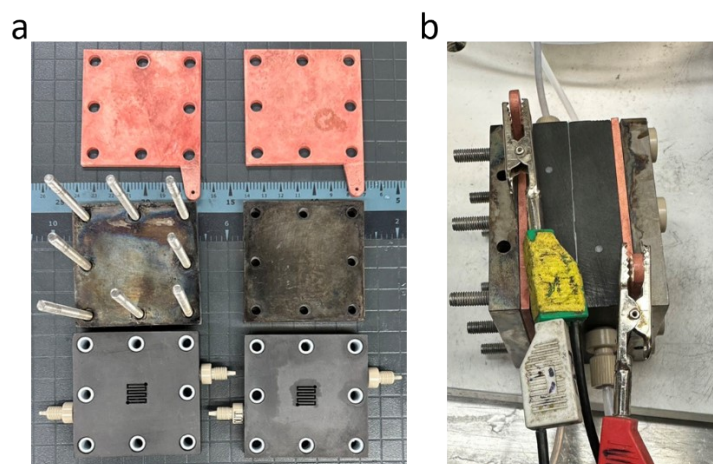


**Figure S17** Photo of the AEM electrolyzer (Model MRT-1). (a) Disassembled and (b) Assembled.

**Table S1.** Comparison with the previous literature on noble metal based hydrazine assisted water electrolyzers

| Materials                                | Electrolyte                                       | Electrolyzer performance   | Reference |
|--|---|--|-----------|
| Ru decorated Ag nanoparticles            | 1.0 M KOH<br>+1.0 M N <sub>2</sub> H <sub>4</sub> | 0.016 V@100 mA/cm <sup>2</sup><br>983±30 mA/cm <sup>2</sup> @0.45V | This work |
| Ultrasmall Ru nanoparticles              | 1.0 M KOH<br>+1.0 M N <sub>2</sub> H <sub>4</sub> | 0.069 V@100 mA/cm <sup>2</sup><br>673±17 mA/cm <sup>2</sup> @0.45V | This work |
| Commercial Ru/C                          | 1.0 M KOH<br>+1.0 M N <sub>2</sub> H <sub>4</sub> | 0.164 V@100 mA/cm <sup>2</sup><br>378±15 mA/cm <sup>2</sup> @0.45V | This work |
| RhRu <sub>0.5</sub> alloy wavy nanowires | 1.0 M KOH<br>+1.0 M N <sub>2</sub> H <sub>4</sub> | 0.054 V@100 mA/cm <sup>2</sup><br>853 mA/cm <sup>2</sup> @0.6V     | [5]       |
| RhPb nanoflowers                         | 1.0 M KOH<br>+0.5 M N <sub>2</sub> H <sub>4</sub> | 0.095 V@10 mA/cm <sup>2</sup><br>0.321 V@100 mA/cm <sup>2</sup>    | [6]       |
| mesoporous RhIr NPs                      | 1.0 M KOH<br>+0.5 M N <sub>2</sub> H <sub>4</sub> | 0.13 V@10 mA/cm <sup>2</sup><br>0.604 V@100 mA/cm <sup>2</sup>     | [7]       |
| Ru/MPNC                                  | 1.0 M KOH<br>+0.5 M N <sub>2</sub> H <sub>4</sub> | 0.149 V@50 mA/cm <sup>2</sup><br>350 mA/cm <sup>2</sup> @0.5V      | [8]       |
| Ru/PNC                                   | 1.0 M KOH<br>+0.5 M N <sub>2</sub> H <sub>4</sub> | 0.19 V@100 mA/cm <sup>2</sup><br>330 mA/cm <sup>2</sup> @0.5V      | [9]       |
| Ru SAs@WS <sub>2</sub> /CC               | 1.0 M KOH<br>+0.5 M N <sub>2</sub> H <sub>4</sub> | 0.0154 V@10 mA/cm <sup>2</sup><br>0.31V@200 mA/cm <sup>2</sup>     | [10]      |
| RuP <sub>2</sub> /CPM                    | 1.0 M KOH<br>+0.3 M N <sub>2</sub> H <sub>4</sub> | 0.023 V@10 mA/cm <sup>2</sup><br>522 mA/cm <sup>2</sup> @1.0V      | [11]      |
| Rh/RhO <sub>x</sub> nanosheet            | 1.0 M KOH<br>+0.5 M N <sub>2</sub> H <sub>4</sub> | 0.068 V @10 mA/cm <sup>2</sup><br>0.279 V@100 mA/cm <sup>2</sup>   | [12]      |
| Au@Rh core@shell nanowire                | 1.0 M KOH<br>+0.1 M N <sub>2</sub> H <sub>4</sub> | 0.18 V@10 mA/cm <sup>2</sup>                                       | [13]      |
| Rh/N-CBs                                 | 1.0 M KOH<br>+0.5 M N <sub>2</sub> H <sub>4</sub> | 0.2 V@10 mA/cm <sup>2</sup>  | [14]      |

## References

- [1] J. P. Perdew, K. Burke, M. Ernzerhof, *Phys Rev Lett* **1996**, *77*, 3865-3868.
- [2] S. Gautier, S. N. Steinmann, C. Michel, P. Fleurat-Lessard, P. Sautet, *Phys Chem Chem Phys* **2015**, *17*, 28921-28930.
- [3] G. Kresse, D. Joubert, *Physical Review B* **1999**, *59*, 1758-1775.
- [4] G. Henkelman, B. P. Uberuaga, H. Jónsson, *The Journal of Chemical Physics* **2000**, *113*, 9901-9904.
- [5] X. Y. Fu, D. F. Cheng, C. Z. Wan, S. Kumari, H. T. Zhang, A. Zhang, H. Huyan, J. X. Zhou, H. Y. Ren, S. B. Wang, Z. P. Zhao, X. Zhao, J. Chen, X. Q. Pan, P. Sautet, Y. Huang, X. F. Duan, *Adv. Mater.* **2023**.
- [6] W. J. Tian, X. Zhang, Z. Q. Wang, L. Cui, M. Li, Y. Xu, X. N. Li, L. Wang, H. J. Wang, *Chem. Eng. J.* **2022**, *440*.
- [7] M. Zhang, Z. Q. Wang, Z. Y. Duan, S. Q. Wang, Y. Xu, X. N. Li, L. Wang, H. J. Wang, *J. Mater. Chem. A* **2021**, *9*, 18323-18328.
- [8] J. S. Wang, X. Y. Guan, H. B. Li, S. Y. Zeng, R. Li, Q. X. Yao, H. Y. Chen, Y. Zheng, K. G. Qu, *Nano Energy* **2022**, *100*.
- [9] X. Y. Guan, Q. N. Wu, H. B. Li, S. Y. Zeng, Q. X. Yao, R. Li, H. Y. Chen, Y. Zheng, K. G. Qu, *Appl. Catal. B-Environ.* **2023**, *323*.
- [10] J. C. Li, Y. Li, J. A. Wang, C. Zhang, H. J. Ma, C. H. Zhu, D. D. Fan, Z. Q. Guo, M. Xu, Y. Y. Wang, H. X. Ma, *Adv. Funct. Mater.* **2022**, *32*.
- [11] Y. P. Li, J. H. Zhang, Y. Liu, Q. Z. Qian, Z. Y. Li, Y. Zhu, G. Q. Zhang, *Sci. Adv.* **2020**, *6*, abb4197.
- [12] J. J. Yang, L. Xu, W. X. Zhu, M. Xie, F. Liao, T. Cheng, Z. H. Kang, M. W. Shao, *J. Mater. Chem. A* **2022**, *10*, 1891-1898.
- [13] Q. Xue, H. Huang, J. Y. Zhu, Y. Zhao, F. M. Li, P. Chen, Y. Chen, *Appl. Catal. B-Environ.* **2020**, *278*, 10.
- [14] N. Jia, Y. P. Liu, L. Wang, P. Chen, X. B. Chen, Z. W. An, Y. Chen, *ACS Appl. Mater. Interfaces* **2019**, *11*, 35039-35049.